

Monitoring impacts of ecological engineering on ecosystem services with geospatial techniques in karst areas of SW China

Min Liu, Xiaoyong Bai, Qiu Tan, Guangjie Luo, Cuiwei Zhao, Luhua Wu, Zeyin Hu, Chen Ran & Yuanhong Deng

To cite this article: Min Liu, Xiaoyong Bai, Qiu Tan, Guangjie Luo, Cuiwei Zhao, Luhua Wu, Zeyin Hu, Chen Ran & Yuanhong Deng (2021): Monitoring impacts of ecological engineering on ecosystem services with geospatial techniques in karst areas of SW China, Geocarto International, DOI: [10.1080/10106049.2021.1903580](https://doi.org/10.1080/10106049.2021.1903580)

To link to this article: <https://doi.org/10.1080/10106049.2021.1903580>



Published online: 05 Apr 2021.



Submit your article to this journal [↗](#)



Article views: 93




View related articles [↗](#)



View Crossmark data [↗](#)



Monitoring impacts of ecological engineering on ecosystem services with geospatial techniques in karst areas of SW China

Min Liu^{a,b}, Xiaoyong Bai^{b,c,d} , Qiu Tan^a, Guangjie Luo^e, Cuiwei Zhao^a,
Luhua Wu^{b,c,d}, Zeyin Hu^{b,c,d}, Chen Ran^{a,b} and Yuanhong Deng^{b,c,d}

^aSchool of Geography and Environmental Sciences, Guizhou Normal University, Guiyang, China; ^bState Key Laboratory of Environmental Geochemistry, Institute of Geochemistry, Chinese Academy of Sciences, Guizhou Province, Guiyang, China; ^cCAS Center for Excellence in Quaternary Science and Global Change, Shanxi Province, Xi'an, China; ^dPuding Karst Ecosystem Observation and Research Station, Chinese Academy of Sciences, Guizhou Province, Puding, China; ^eGuizhou Provincial Key Laboratory of Geographic State Monitoring of Watershed, Guizhou Education University, Guiyang, China

ABSTRACT

Ecosystem services (ESs) synergies have been broadly studied, whose synergy control areas and driving mechanisms were still not fully understood. Here, We analyzed soil conservation (SC), water yield (WY), net primary productivity (NPP) and food supply (FS) on the basis of geospatial analysis techniques from 1992 to 2015. The results showed that the SW karst areas contributed 23.7% of SC and 14.56% of NPP with only 8.4% of China's continent. 49.28% of China's land was synergy control areas, while accounted for 82.23% in the SW karst areas. The cause of this phenomenon was twofold, one was the significant increase in NDVI was mainly due to human activities (HA), and the coincidence rates between the HA dominated areas and the synergies control areas up to 90.7%. These results emphasized that ecological engineering was a key factor of the synergy among multi-ESs, the synergy control areas should be priority for ecological restoration.

ARTICLE HISTORY

Received 24 December 2020
Accepted 20 February 2021

KEYWORDS

Ecosystem services; NPP; synergies; karst; ecological engineering

1 Introduction

Ecosystem services (ESs) were defined as the benefits people receive from ecosystems (Guerry 2015), it directly or indirectly affects human well-being and ecological security (Costanza et al. 1997). It was reported that classification of ESs was proposed by The Millennium Ecosystem Assessment (MA 2005), which was classified into four types: production services, regulation services, cultural services, and support services. This classification had spawned extensive research on developing a classification scheme for ES (Ouyang et al. 1999). The contribution of the degradation of natural resources to human well-being had not been fully understood and underestimated, and it will lead to

ecosystem change and a decline in the material basis for human survival (Lele et al. 2013), Therefore, the ES assessment was an important scientific topic for sustainable development (Bai et al. 2018). One ES change will be accompanied by another ESs change, the trade-offs and synergies of ES are formed (Howe et al. 2014; Qin et al. 2015; Ran et al. 2019). If the government focuses on the restoration of single ES and ignores the trade-offs and synergies among ES, it may lead to deterioration of the ecological environment (Diaz and Rosenberg 2008). With the rapid development of society and the economy, the ecological environment is facing great challenges. Research on trade-offs and synergies of ESs and the factors clarifying was the basis and prerequisites for achieving sustainable development (Goldstein et al. 2012; Pan et al. 2013; Peng et al. 2019; Zheng et al. 2019; Sun et al. 2019).

In recent years, research on the trade-offs and synergy of ESs had become the focus of research in related disciplines. The recent literature and comprehensive methodological guidelines for assessing the trade-offs between each of ESs were first proposed by Mouchet et al. (2014) and others. Howe conducted a comprehensive analysis of ESs relationships (Howe et al. 2014), reveals how environmental or social conditions produced tradeoffs between each of ESs; the trade-offs and the spatial distribution of ecosystem services were determined by historical and socio-ecological in Danish (Turner et al. 2014); There was a clear interaction between FS and local climate in sub-Saharan Africa (Palm et al. 2010); a study on Beijing of China, predicted the potential changes in future ESs (Bai et al. 2012). At the same time, more and more research on ESs changes with land use changes (Barbier et al. 2008); land use types were considered as aggregations including different physicochemical conditions and geochemical processes (Liu and Han 2020). Land use change was considered to be the main influencing factor to change ES which could affect the ES by regulating land policies to achieve the purpose of regional development (Simonit and Perrings 2013; Tian et al. 2016; Xu et al. 2018; Santiago and José Luis 2019), and reduce the impact of trade-offs between ESs (Yang et al. 2018), even be transformed into synergies (Bennet et al. 2009; Renard et al. 2015; Wu et al. 2017). On the other hand, the results of assessment the ES could conducive to land use planning (Bai et al. 2018). The large-scale conversion of land use mostly comes from the role of ecological engineering. Some studies have quantified the impact of environmental engineering on the local ecological environment (Lü et al. 2012; Li et al. 2016; Tong et al. 2017; Zhang et al. 2018; Chen et al. 2019; Liu et al. 2020). Due to population growth and economic activity, 60% of the global ESs had been degraded (Joppa et al. 2016), and ecological engineering had a positive impact on improving ESs (Zhang et al. 2018).

Although significant progress on ES had been made, there were still present some limitations to be resolved. Previous research was limited to a local scale, the research in different geographical divisions was unclear from the perspective of regional differences; lacked spatial expression of intra-regional spatiotemporal differences; lacked exploration of the trade-offs and synergies among multiple ESs, hard to identify key and efficient restoration areas and its driving mechanism. The impact of environmental engineering on the trade-offs and synergies of ecosystem services was also unclear.

Above question greatly hinders to understanding of the trade off and synergy of ecosystem services in China. So, this study analyzed the spatiotemporal characteristics and trade off and synergy of SC, WY, NPP, and FS from 1992 to 2015 in China. We have addressed the following scientific issues: (1) The change trend and spatial pattern of four ecosystem services in China were analyzed. (2) The interaction of multiple ESs in China was determined By superimposing the correlations of ESs, and considering the regional

differences, We analyzed the strength of ES relationship in nine agricultural divisions of China. (3) Clarified the role of climate change and human activities on vegetation restoration and the synergy among multiple ESs in the southwest karst region. The main influencing factors of the synergy among multiple ESs in karst area of Southwest China were confirmed by exploring the test of mutation year and the spatial coincidence rate of vegetation restoration area and multi-ESs synergy areas controlled by human activities.

In summary, Our research revealed the changes of ES in China and clarified future ecological development strategies, and identified the strength of ES relations and correlation levels in nine agricultural divisions of China. Linking ecosystem services synergies, hotspot identification with Human activity dominated vegetation restoration areas in China. This finding will help to identify areas with efficient ecological restoration. This is what other articles lack. The multi-ESs ascending and degrading areas and their driving mechanisms have been identified from regional scale, accurately identify and control key sensitive links of ecosystem services to promote overall collaborative improvement (Goldstein et al. 2012).

2 Materials and methods

2.1. Data source

GIMMS NDVI, which was obtained by NOAA's high resolution radiometric sensor, was widely used to study large-scale vegetation phenological changes (Zhou et al. 2001; Slayback et al. 2003; Zeng et al. 2017; Yang et al. 2019).

Meteorological data on precipitation and temperature were obtained from more than 2400 weather stations daily observation data, which was produced by the China meteorological science data sharing network. ANUSPLIN interpolation software was used for statistical analysis and data diagnosis, and the spatial distribution of data was analyzed to achieve spatial interpolation. Sun radiation and drought index were came from Terrestrial Hydrology Research Group of Princeton University. Calculation of the evapotranspiration potential in the Standardized Precipitation-Evapotranspiration Index (SPEI) was based on the FAO-56 Penman-Monteith method. The SPEI base, offers long-time, robust information on the drought conditions at the global scale. It providing SPEI time-scales between 1 and 48 months. This article uses data processing based on 12 months.

Soil data was constructed by the Food and Agriculture Organization of the United Nations (FAO) and the Vienna International Institute for Applied Systems (IIASA, 1.1), the data source in China was 1: 1 million soil data provided by Nanjing Soil of the Second National Land Survey. The projection format was WGS84 and the soil classification system used was mainly FAO-90 (Tifafi et al. 2017).

Land use data derived from the European Space Agency Climate Change Initiative dataset. The NPP was produced by the Chinese land-based monthly meteorological data, national soil texture data, and land cover and vegetation index data based on MODIS and AVHRR remote sensing images through the CASA model. Relevant research results based on this data set have been published in 'Remote sensing' (Chen 2019). In this article, all method was conducted at the pixel level ($0.05^\circ \times 0.05^\circ$) to detected the spatiotemporal evolution of ES in order to ensure data matching and operation. The vector boundaries of nine agricultural subregions in China used in this article were from the Resource and Environment Science and Data Center, and the SW Karst region boundary were considered by the regional boundary of Tong (Tong et al. 2017, 2018), and this boundary was

Table 1. Data sources and description of this study.

Date name	Date description	Date source
DEM	Raster; 1 km × 1 km	http://www.gscloud.cn
GIMMS NDVI	Raster; 8 km × 8 km	https://www.noaa.gov/
Socio-economic data	Statistics	http://www.stats.gov.cn
Meteorological data	Raster; 1 km × 1 km	http://data.cma.cn
Soil data	Raster; 1 km × 1 km	http://www.fao.org/ https://www.omicsonline.org/ http://data.tpdc.ac.cn
land use data	Raster; 0.3 km × 0.3 km	https://www.esa-landcover-cci.org/
NPP	Monthly continental	http://www.resdc.cn/
Sun radiation	1 km × 1 km	http://hydrology.princeton.edu/home.php
Standardized Precipitation-Evapotranspiration Index	1 km × 1 km	http://digital.csic.es/handle/10261/153475
China's nine major agricultural divisions	Vector border	http://www.resdc.cn/

consistent with The Yunnan-Guizhou Plateau in the nine major agricultural areas, so we usually call it the ‘Southwest Karst Region’ in the research (Table 1).

2.2. Analysis method

The framework and structure used in this research were shown in Figure 1, and various methods were also described in detail.

2.2.1. Soil conservation model

The model of RUSLE (Renard et al. 1997) had a wide range of uses and strong operability in estimated soil retention.

$$A_m = R \times K \times L \times S \times C \times P \quad (1)$$

$$A_p = LS \times K \times R \quad (2)$$

$$A_c = A_p - A_m \quad (3)$$

$$R = \sum_{i=1}^{12} (-1.5527 + 0.1792P_i) \quad (4)$$

$$C = \begin{cases} 1(\beta = 0) \\ 0.6508 - 0.3436 \times \beta & (0 < \beta \leq 78.3\%) \\ 0(\beta > 78.3\%) \end{cases} \quad (5)$$

$$\beta = \frac{(NDVI - NDVI_{\min})}{(NDVI_{\max} - NDVI_{\min})} \quad (6)$$

$$LS = \left(\frac{\lambda}{22.13} \right)^n (65.41 \sin^2 \theta + 4.56 \sin \theta + 0.065) \quad (7)$$

$$K = \left\{ 0.2 + 0.3 \exp \left[-0.0256 S_d \left(1 - \frac{S_i}{100} \right) \right] \right\} \left(\frac{S_i}{C_i + S_i} \right)^{0.3} \left[1 - \frac{0.25 C_{or}}{C_{or} + \exp(3.72 - 2.95 C_{or})} \right] \left[1 - \frac{0.7(1 - S_d)}{1 - S_d + \exp(-5.51 + 22.9(1 - S_d))} \right] \quad (8)$$

A_m was the average actual soil loss ($t \cdot hm^{-2} \cdot a^{-1}$), A_p was the average potential soil loss, and A_c was the average soil retention, R was the precipitation erosivity factor

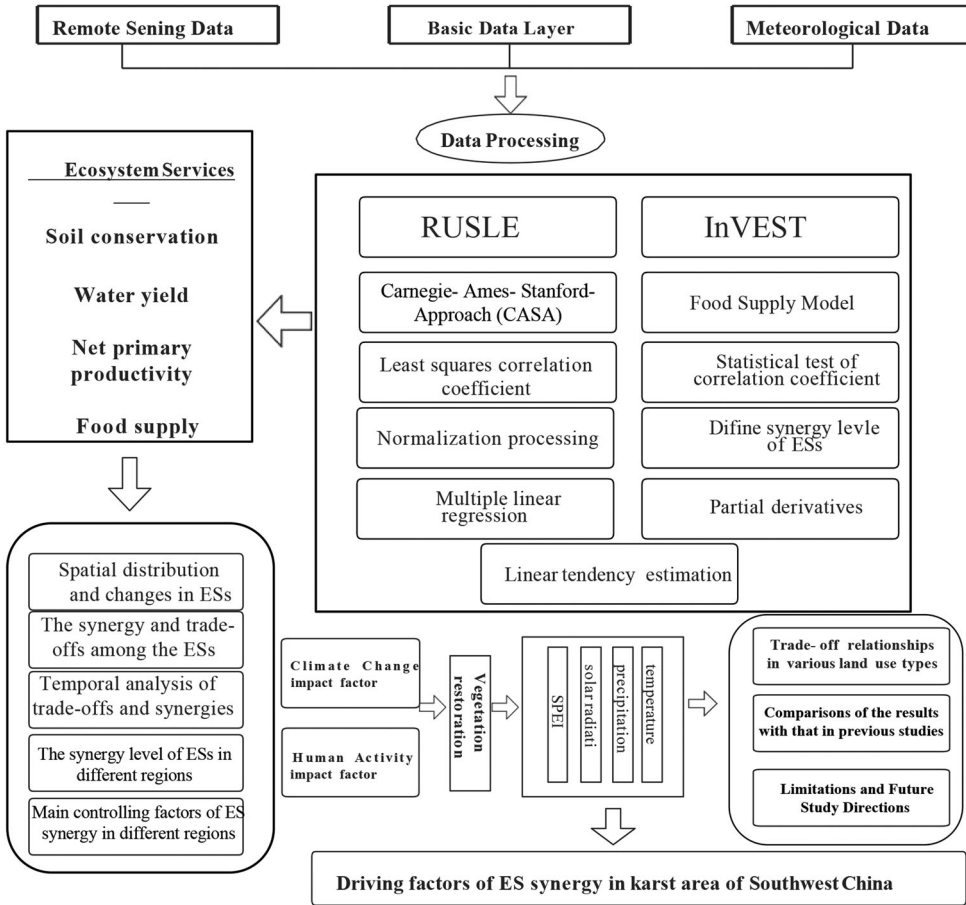


Figure 1. Framework and program diagram.

(Wischmeier 1971; Pan et al. 2010), K was the soil erodibility factor, L was the slope length, S was the factor of slope (McCool et al. 1989; Liu et al. 2000), C was the factor of crop cover and management (Cai 2000), P was the factor of soil conservation measure (Sun et al. 2014, Zeng et al. 2017). P_i was the precipitation in the i th month, β was the vegetation coverage, S_d was sand content (%), S_i was powder content (%), C_i was clay content, C_{or} was surface soil organic carbon content(%) (Williams and Arnold 1997).

2.2.2. Water yield model

The evaluation of the water yield was based on the InVEST model (Wang et al. 2016) and Budyko curve, This method considers the influence of rainfall and evapotranspiration on water yield (Gong et al. 2017). The equation was:

$$TQ = \left(1 - \frac{P}{ET}\right) \times P \times Ai \quad (9)$$

$$\frac{AET(x)}{P(x)} = 1 + \frac{PET(x)}{P(x)} - \left[1 + \left(\frac{PET(x)}{P(x)}\right)^w\right]^{1/w} \quad (10)$$

$$PET(x) = K_c(x) \times ET_o(x) \quad (11)$$

$$w(x) = \frac{AWC(x) \times Z}{P(x)} + 1.25 \quad (12)$$

TQ was the total water source conservation (m^3), P was the annual rainfall (mm), ET was the evapotranspiration, and A_i was the area of a single pixel. $PET(x)$ was the potential evapotranspiration of grid unit x ; $ET_o(x)$ was the reference vegetation evapotranspiration; $KC(x)$ was the crop evapotranspiration coefficient; $AWC(x)$ was the available water content of plants; $w(x)$ was the Empirical parameter; Z was the Zhang coefficient (Zhang et al. 2004).

2.2.3. NPP model

This article used the CASA mode to estimate the value of NPP (Potter et al. 1993), The equation was:

$$NPP(x, t) = APAR(x, t) \times \varepsilon(x, t) \quad (13)$$

$APAR(x, t)$ represents the photosynthetically active radiation ($MJ \cdot m^{-2}$) absorbed by the spatial position x in time t ; $\varepsilon(x, t)$ represents the actual light energy utilization of the pixel x in time t ($g \cdot C/MJ$).

2.2.4. Food supply model

Analyzed the spatial distribution of FS combined the land use cover and statistical year-book data (Sun et al. 2020). Calculated as follows:

$$G_i = A_i \times N_i \quad (14)$$

$$N_i = F_i / S_i \quad (15)$$

where G_i was the amount of i th food for each pixel (t/ha), A_i was the area of the land use type corresponding to various foods i th (km^2), N_i was the supply of i th food for the unit area (t/km^2), F_i was the total supply (t/yr), and S_i was the total areas of i th food (km^2). In general, we correspond agricultural products belong to the cultivated field, forest products belong to the woodland, the output of meat and milk belong to the grassland, and aquatic products belong to the waters.

2.2.5. Trade-off and synergistic correlation analysis statistical methods

ES was complex. In the same region, changes in one ES will inevitably lead to changes in another ES or even multi-ESs (Bennett et al. 2009; Li et al. 2013; Sun et al, 2019). Therefore, it was necessary to eliminate the influence of unrelated factors. Analyze the relationship between the each ESs, namely the correlation analysis. Calculated as follows:

$$r_{12(ij)} = \frac{\sum_{n=1}^n (ES1_{n(ij)} - \overline{ES1}_{(ij)}) (ES2_{n(ij)} - \overline{ES2}_{(ij)})}{\sqrt{\sum_{n=1}^n (ES1_{n(ij)} - \overline{ES1}_{(ij)})^2 \sum_{n=1}^n (ES2_{n(ij)} - \overline{ES2}_{(ij)})^2}} \quad (16)$$

where r_{12} was the spatial correlation coefficient whose values ranged from -1 to 1 . The region with $r_{12} > 0$ indicates that the two ES were collaborative, that was the positive correlation between two variables, and vice versa. The higher the value of r_{12} , the stronger the relationship between them.

2.2.6. The synergy level of ESs

We performed spatial overlay operations for ESs layers with Geospatial Techniques, and recognized the interactions among multiple ESs by interpreting the codes in the pixels of the output layers of overlay analysis. For example, code 1 and 2 indicates that synergy and trade-off, code '112121' indicates that synergy area for four ecosystem services and trade-offs with the two services. Code '111111' indicates that all ESs were synergies, and the regions as extreme synergy areas. We summarize all the cases and obtained seven different grades.

2.2.7. Sensitivity of vegetation restoration on climate changes

The sensitivity of NDVI to changes in Climate change was computed for the whole 1992–2015 period. It was expressed as the partial derivative that results from a multiple linear regression, where ΔNDVI , ΔT , ΔP , ΔSR and ΔSPEI represent the linear trend of the NDVI, annually averaged temperature, precipitation, solar radiation and drought index variations, respectively (Forzieri et al. 2020).

$$\Delta\text{NDVI} = \frac{\sum_{i=1}^n (i \times \text{NDVI}_i) - \frac{1}{n} \sum_{i=1}^n i \times \sum_{i=1}^n \text{NDVI}_i}{\sum_{i=1}^n i^2 - \frac{1}{n} (\sum_{i=1}^n i)^2} \quad (17)$$

$$\Delta\text{NDVI} = \text{HA}_{\text{con}} + \text{CC}_{\text{con}} = \text{HA}_{\text{con}} + \delta P^{\text{NDVI}} + \delta T^{\text{NDVI}} + \delta \text{SR}^{\text{NDVI}} + \delta \text{SPEI}^{\text{NDVI}} \quad (18)$$

$$\delta P^{\text{NDVI}} = \frac{\partial \text{NDVI}}{\partial P} \Delta P \quad (19)$$

$$\Delta\text{NDVI} = \beta_0 + \frac{\partial \text{NDVI}}{\partial P} \Delta P + \frac{\partial \text{NDVI}}{\partial T} \Delta T + \frac{\partial \text{NDVI}}{\partial \text{SR}} \Delta \text{SR} + \frac{\partial \text{NDVI}}{\partial \text{SPEI}} \Delta \text{SPEI} \quad (20)$$

where n represents the 24-year time span from 1992–2015, NDVI_i was the annual NDVI value of year i . At the same time, we used the same method to analyze the trends of T , P , SR , and SPEI . The derived signal $\frac{\partial \text{NDVI}}{\partial P}$ integrates the bidirectional interactions between P and the NDVI term, the $\frac{\partial \text{NDVI}}{\partial T}$ integrates between T and the NDVI term, the $\frac{\partial \text{NDVI}}{\partial \text{SR}}$ integrates between T and the NDVI term, the $\frac{\partial \text{NDVI}}{\partial \text{SPEI}}$ integrates between T and the NDVI term, all predictors in Eq. (20) were quantified for each pixel over a centered $1 \text{ km} \times 1 \text{ km}$ spatial window.

In order to further distinguish the influence of climate and human activities on NPP trends, the relative effects of ecological restoration projects are calculated according to the formula in Table 2 (divided into four scenarios).

Table 2. Four scenarios for quantitatively assessing the contribution proportions of climate-and human-controlled NDVI increasing.

	Scenario	CC_con	HA_con	Contribution proportion of CC(%)	Contribution proportion of HA(%)
NDVI increasing	1	>0	>0	$\frac{ \text{CC}_{\text{con}} }{ \text{CC}_{\text{con}} + \text{HA}_{\text{con}} } \times 100$	$\frac{ \text{HA}_{\text{con}} }{ \text{CC}_{\text{con}} + \text{HA}_{\text{con}} } \times 100$
	2	>0	<0	100	0
	3	<0	>0	0	100
	4	<0	<0	Error	Error

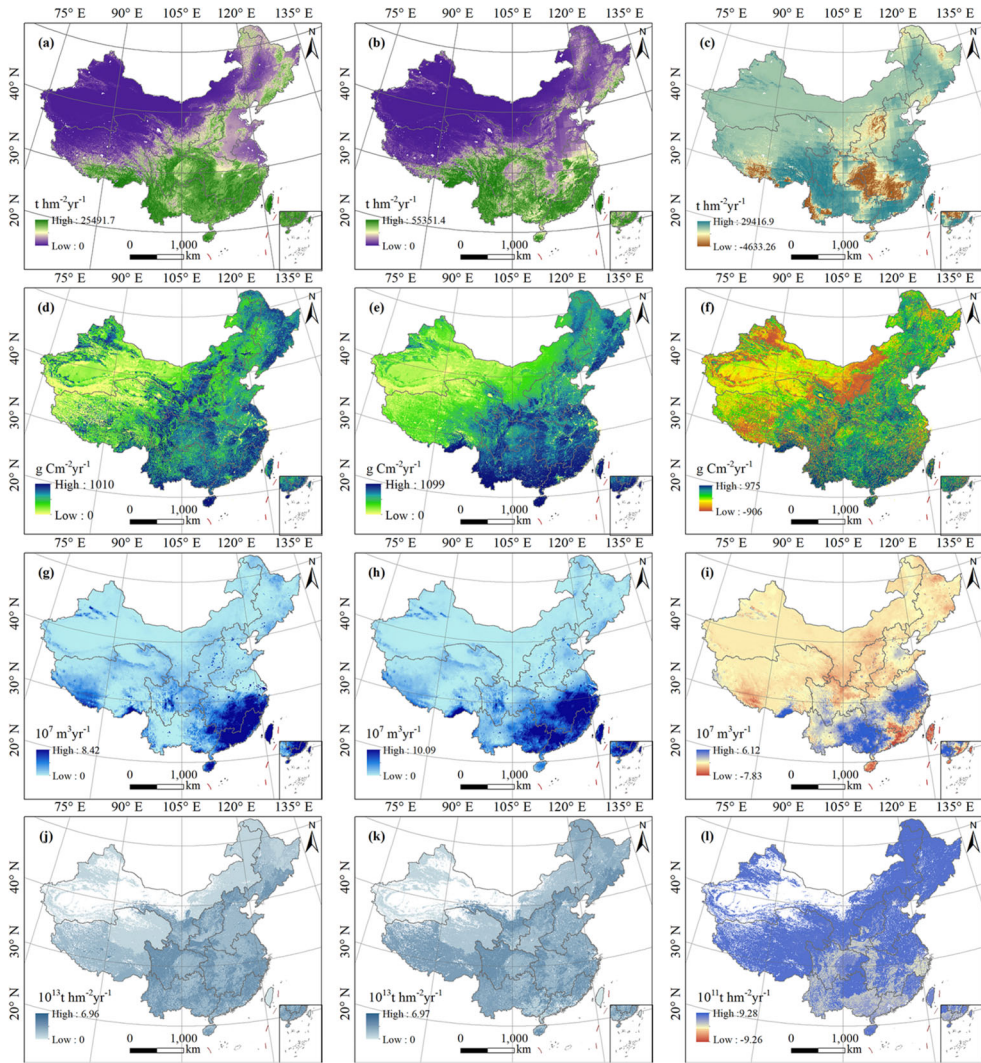


Figure 2. The synergy level of ESs diagram. This region was the extreme synergy if all ESs in a region were synergistic, otherwise, it was the extreme trade-off. The pie chart is the areas ratio of 7 levels. The 1, 2, 3, 4, 5, 6 in (a–i) correspond to the legend in the main picture; (a) Northern arid and semiarid region; (b) Northeast China Plain; (c) Qinghai Tibet Plateau; (d) Sichuan Basin and surrounding regions; (e) Loess Plateau; (f) Huang-Huai-Hai Plain; (g) Middle-lower Yangtze Plain; (h) Karst areas in southwest China; (i) Southern China.

3 Results

3.1. Spatial distribution and changes in ESs

According to the spatial change of ES in China from 1992 to 2015 (Figure 2), all ESs increased during the evaluation period, and the result was consistent with Ouyang (Ouyang et al. 2016). Among them, The WY, SC, and NPP increased by 33.46%, 24.13%, and 18.63%, respectively. We separately counted the growth rates of FS in four land types, and found that the FS of waters increased by 263.68%, the FS of grassland increased by 142%, the FS of cultivated field increased by 44%, and the FS of woodland increased by

35%. The southwestern karst areas contributed 23.7% of SC (Figure 2(a)), 14.56% of NPP (Figure 2(c)) and 14% of WY (Figure 2(b)) with only 8.4% of China's total land areas. All ESs had increased in the karst areas of southwest China. In addition, the average of NPP and WY increased most rapidly (Table A1). For WY, the karst areas in southwest of China showed the fastest rate of increased ($1.37 \times 10^4 \text{m}^3/\text{km}^2/\text{yr}$) among nine agricultural divisions, but the increase of total WY in SW karst areas was the second largest after the middle-lower Yangtze Plain (total WY increased by $2.86 \times 10^{11} \text{m}^3$).

3.2. The synergy and trade-offs among the ESs

As shown in Figure 3, the spatial distribution characteristics of trade-offs and synergies of ES in China was revealed. There was basically a synergy between the ESs in SW karst areas (Figure 3). The synergy areas between SC and WY accounted for 73.21% of China's total land area (Figure 3(b)), especially concentrated in the karst areas of southwest China (0.42^{***} , $p < 0.01$), Loess Plateau (0.6^{***} , $p < 0.01$) and the middle-lower Yangtze plain (0.36^{***} , $p < 0.01$), the synergies areas accounted for 90.77%, 94.12%, and 74.51% of their land area, respectively.

3.3. Temporal analysis of trade-offs and synergies

The trade-offs and synergies between ES vary greatly over time. Overall, the synergy of SC, NPP, and WY were stronger in the nine agricultural divisions, while the correlation coefficient between FS and other ESs was weak. The ESs correlation coefficient increased the most in the Loess Plateau (Figure 4(e)) and Northern arid and semiarid region (Figure 4(a)). Among them, the synergy between SC and NPP had grown the most significantly in the Loess Plateau (increased of 2.91 times compared with 1992). At the same time, the synergy between SC, NPP and WY both increased suddenly after 2000, the same was true for the synergies between SC and NPP in Northern arid and semiarid region. It can be seen that the increased in woodland brought about by the ecological restoration projects had significantly increased the SC and achieved great effects in these regions. Although the correlation coefficient of ESs was not large in SW Karst areas, but the implementation of the ecological project promoted the synergies relationship between SC and NPP, NPP and WY in the southwest karst area (combined with Figure 5).

3.4. The synergy level of ESs in different regions

According to formula (6), the interaction between multiple ESs is identified according to the number of trade-offs and collaboration relationships, which are divided into seven levels (Figure 5). It could be seen that 49.28% of China's total land areas was synergy control areas (synergy area for more than three ecosystem services in Figure 5) of multi-ESs, and the areas of synergies main control of multi-ESs accounted for 82.23% in SW karst areas (Figure 5(h)). The synergy control areas in SW karst areas was much higher than other areas. The greater the area ratio with higher synergy level of ESs, while the areas with a higher synergy level had a small proportion in other regions (Figure 5(h)). The synergy control areas were regarded as an area where ecological restoration projects could achieve significant results, and it could promote the common improvement of multiple ESs. The synergy control areas should become a key areas for ecological construction. The key sensitive links should be accurately identified and controlled as early as possible to promoted

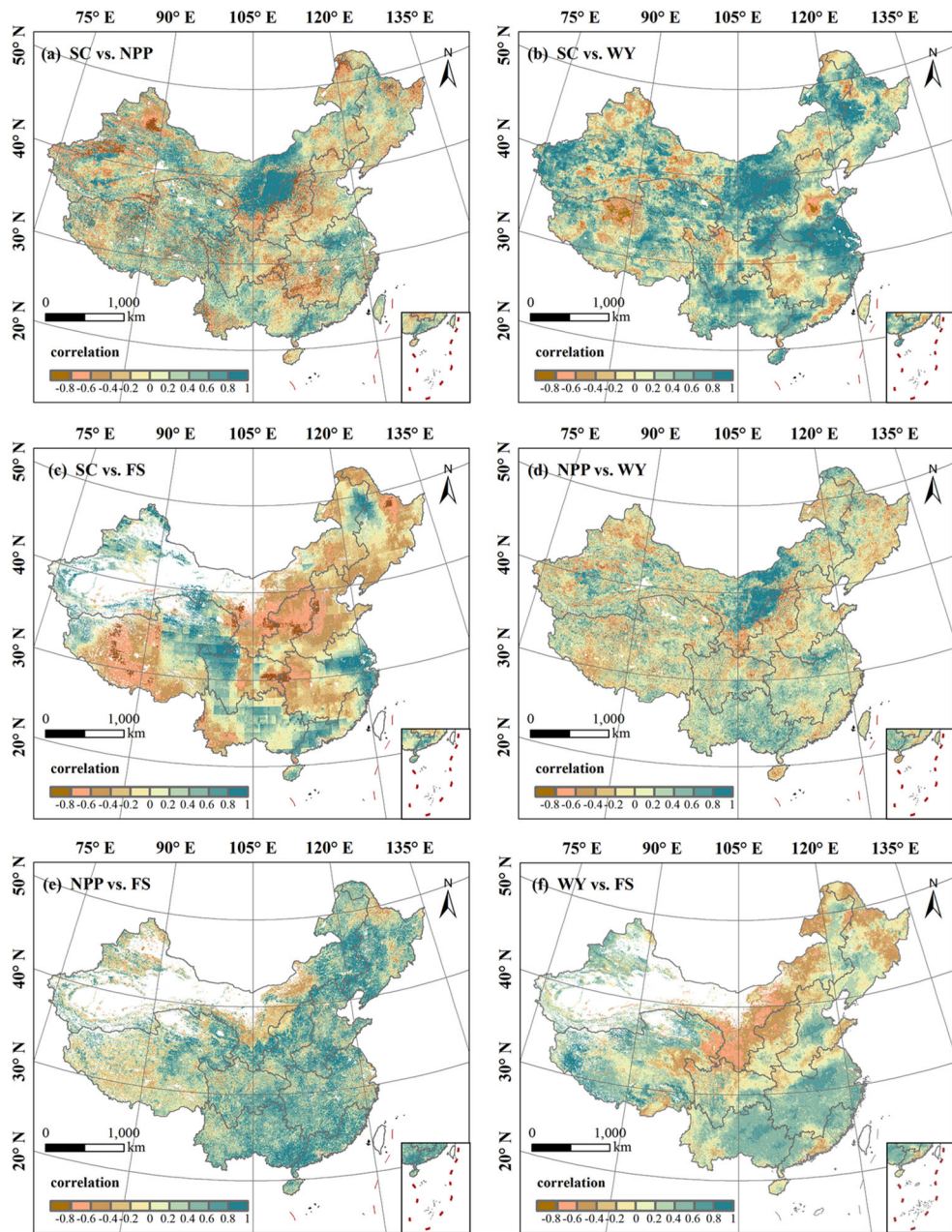


Figure 3. Spatial change map of Soil conservation in 1992 (a), 2015 (b) and changed (c), the Net Primary Productivity in 1992 (d), 2015 (e) and changed (f), the Water yield in 1992 (g), 2015 (h) and changed (i), the Food supply in 1992 (j), 2015(k) and changed (l).

the synergy of ES improvement. This was followed by 63.98% in the middle-lower Yangtze Plain and 63.08% in southern China. In contrast, the Loess Plateau (Figure 5(d)) had stronger trade-off relationship, with the synergy control areas, accounted for only 22.81% of the areas.

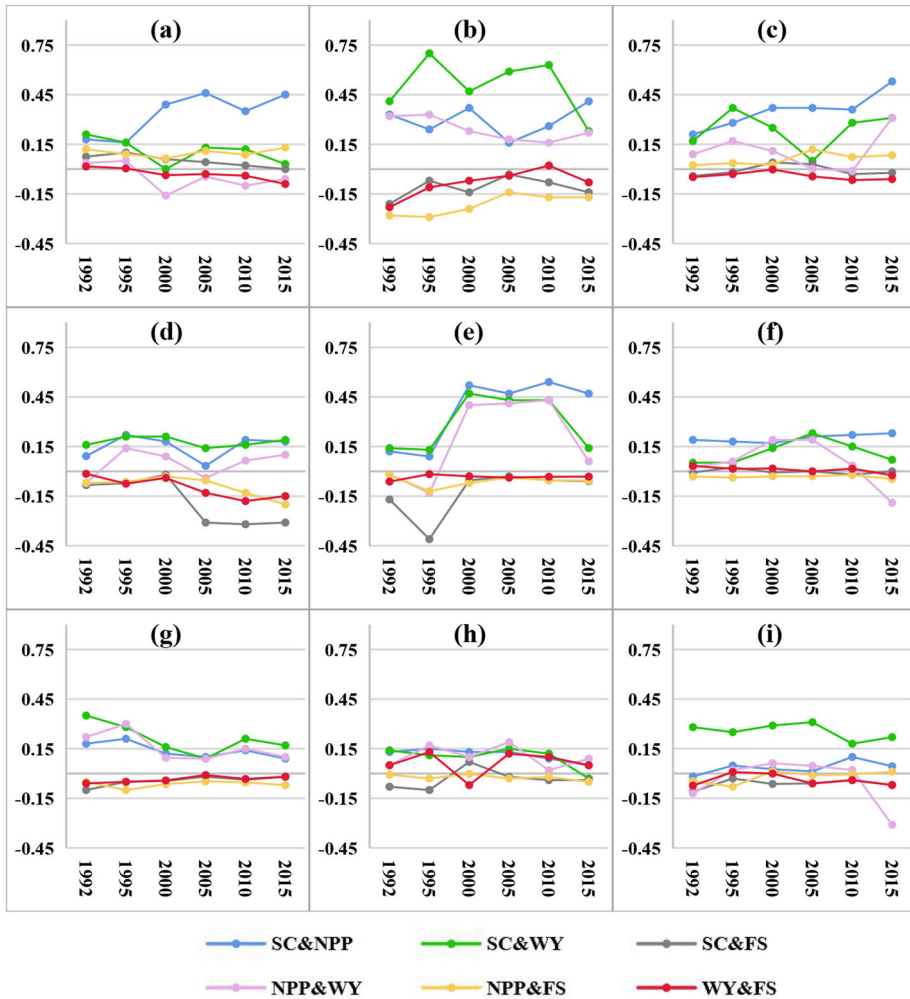


Figure 4. The correlation space map of SC and NPP (a), SC and WY (b), SC and FS (c), NPP and WY (d), NPP and FS (e), WY and FS (f), and correlation level of ES (g).

3.5. Main control factors of ES synergy in different regions

Previous scholars had confirmed that the increase of NDVI could promote the SC and NPP (Peng et al. 2011; Cai et al. 2014; Xiao 2014; Li et al. 2016; Zhang et al. 2016). So, to further identify the dominant areas of each influencing factor, the contribution proportions of climate change (CC) and human activity (HA) for NDVI increased were calculated according to the four designed scenarios in Table 2. For China, the percentages of CC and HA controlled accounted for 61.99% and 38% for NPP increasing (Figure 6(a,b)), respectively. The vegetation restoration trend was mainly controlled by climatic factors in the Northeast Plain, Qinghai-Tibet Plateau, Sichuan Basin, Huanghuaihai Plain, and South China. In contrast, vegetation restoration was controlled by human activities in the Chinese shelterbelt program, such as the Northern arid and semiarid region, the Loess Plateau, the lower reaches of the Yangtze River, and the karst areas in SW China (Figure 6(b)). Figure 4 shown that the synergistic relationship between SC and NPP the Loess

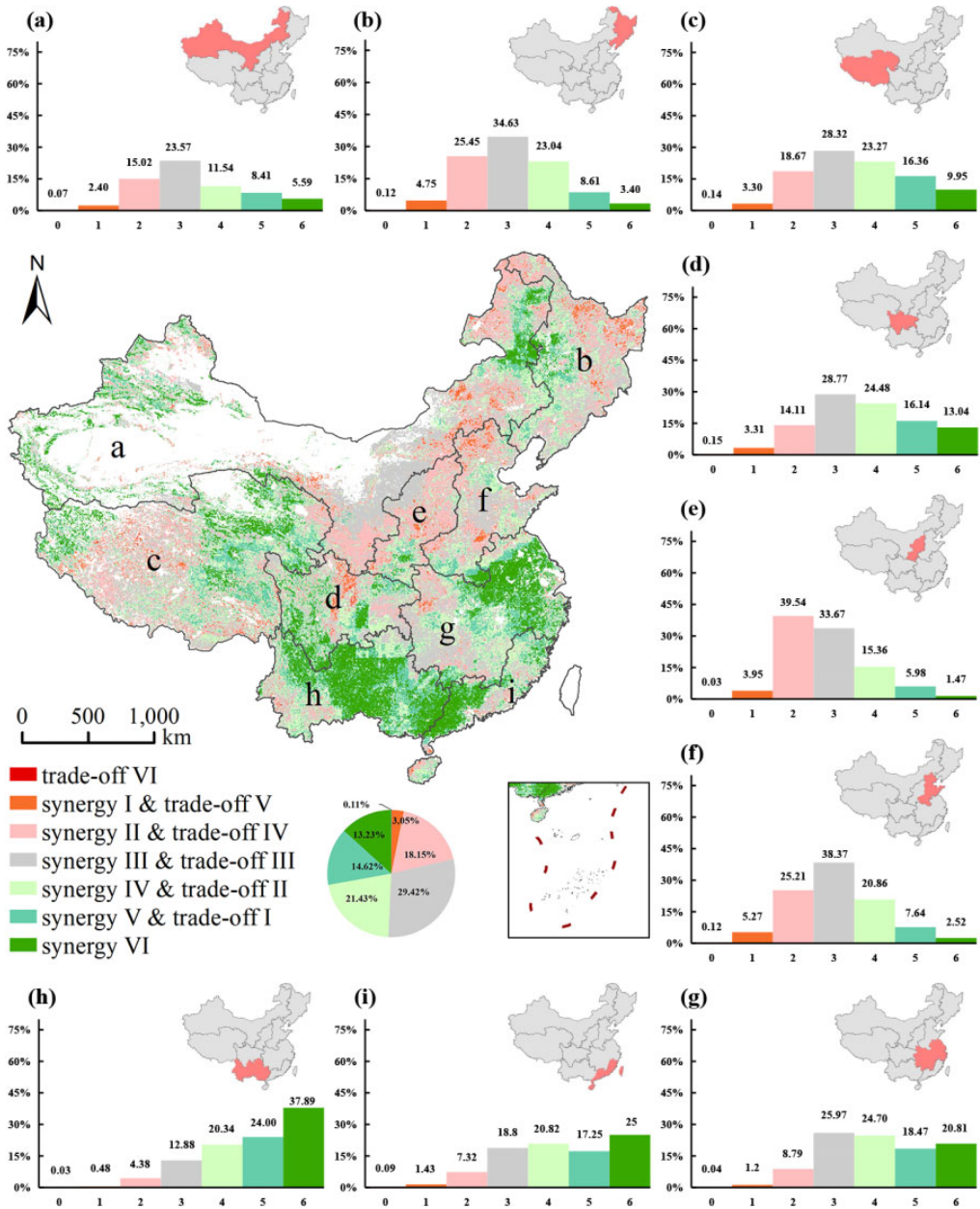


Figure 5. Line chart of correlation coefficients among ES in nine major agricultural districts. (a) Northern arid and semiarid region; (b) Northeast China Plain; (c) Qinghai Tibet Plateau; (d) Sichuan Basin and surrounding regions; (e) Loess Plateau; (f) Huang-Huai-Hai Plain; (g) Middle-lower Yangtze Plain; (h) Karst areas in southwest China; (i) Southern China.

Plateau and the arid and semi-arid regions has increased after 2000. Combined with the Figure 6(e), it can be found that the mutation years of NDVI in the Loess Plateau were concentrated in 2000, and the arid and semi-arid areas in the north were in 2003, due to the positive impact caused by human activities (Figure 6(d)), it can be seen that the

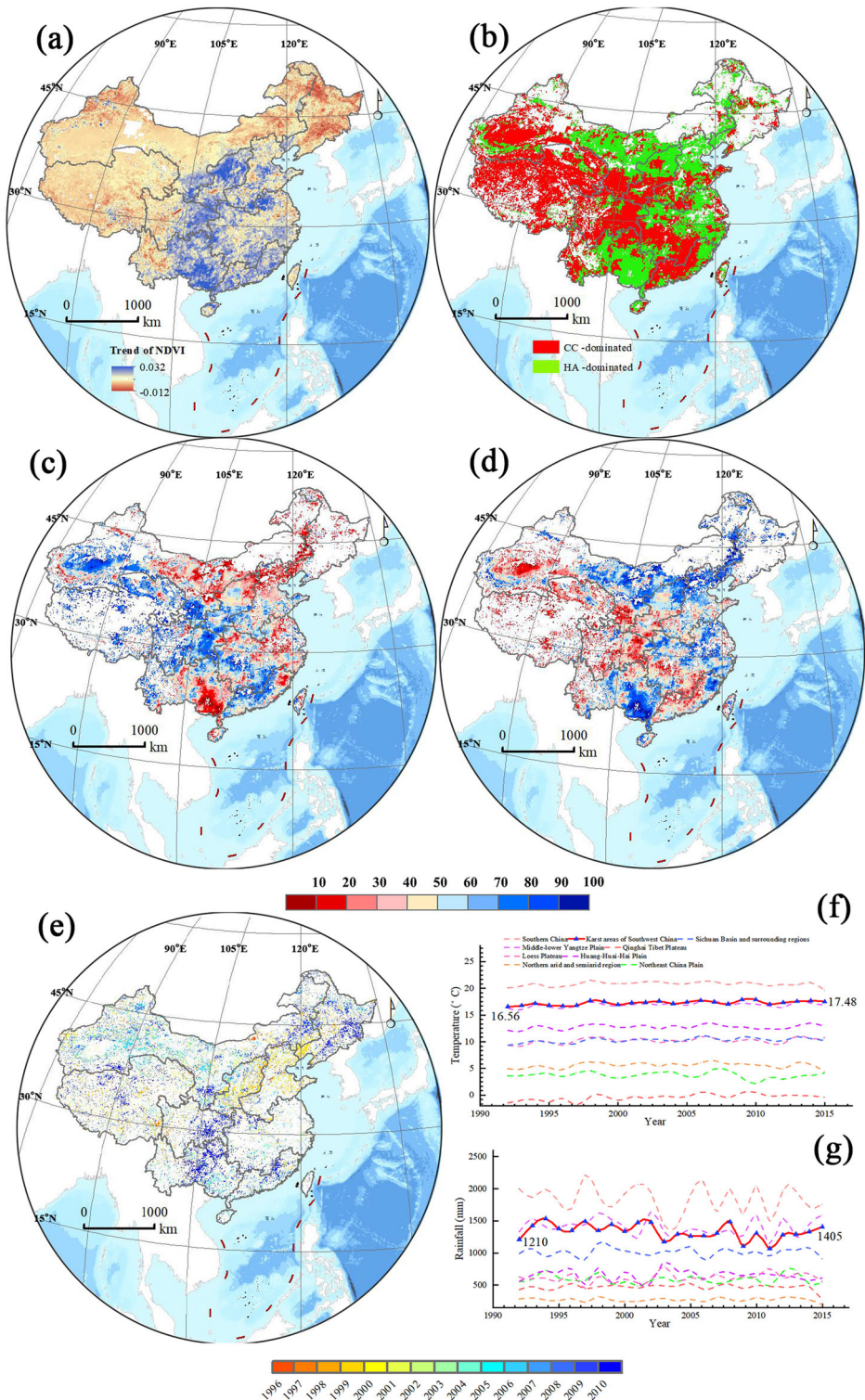


Figure 6. The impact of CC and HA on NPP changes. (a) Trend of NDVI from 1992–2015; (b) Spatial distributions of the climate- and human-dominated NPP increase areas. The contribution proportions that CC (Con_clim) (c) and HA (Con_hum) (d) contributed to NPP increasing; (e) NDVI turning point year spatial distribution map; (f) the average annual temperature line among the nine major divisions; (g) the average annual precipitation line chart among the nine major divisions.

vegetation restoration caused by the implementation of the ecological project had promoted the cooperative relationship between SC and NPP in the two places.

Among all the areas where human activities dominate vegetation restoration, HA dominated the NDVI increased 57.48% in the southwest karst areas (the percentages of HA was highest), which were mainly located in GX, the southern GZ, and the eastern YN. Indeed, We found that NDVI mutation occurred after the implementation of ecological projects (Figure 6(e)). The coverage of NDVI experienced low before the mutation year (Figure A1(a)) and obviously increased after the mutation year (Figure A1(b)), and it was mainly due to human activities. Most important of all, Surprisingly, we found that the overlap rate between the HA dominated areas (Figure 7(b)) and the synergies among ESs areas (Figure 7(a)) was as high as 90.7% (Figure 7(c)), these proved that ecological engineering had played a key role for synergies among multi-ESs synergy in SW karst areas. In addition, Previous research had been confirmed that precipitation showed a positive contribution in NDVI coverage in the karst region of China (Wu et al. 2020), precipitation and temperature were increased trend before and after the mutation year, but the growth rate of precipitation faster than the temperature (Figure 6(f,g)), these promoted the rise of WY. Therefore, SC, NPP, and WY showed synergies in SW karst areas.

4. Discussion

4.1. Trade-off relationships in various land use types

The relationship between ES trade-off and synergy was spatially heterogeneous, which depends to the spatial pattern of land use (Xu et al. 2018). Land use change can cause changes in ES and even ESV (Yang et al. 2018; Hu et al. 2020). The urban land area actively expanded 253%, and wetlands increased by 6.9%. The reduced in unutilized was most pronounced from 1992 to 2015. Cultivated field increased by $5.24 \times 10^4 \text{ km}^2$ from 1992 to 2000, and decreased by $2.96 \times 10^4 \text{ km}^2$ from 2000 to 2015. The woodland decreased before 2000 and then increased (Table 3). It can be found that China's ecological engineering had achieved corresponding results (Lai et al. 2016).

We found that all ES showed an increasing trend in cultivated field and woodland by exploring the dynamic changes of ES under different land use types (Figure 8). The decreased in cultivated field area and the increased in FS output were still may due to the increase in the yield of crops by fertilization, the rapid development of hybrid varieties (Jain 2010; Chen et al. 2019). Nearly three quarters (72.88%) of the synergy came from cultivated field and grassland (37.06% of cultivated land, 35.08% of woodland, Figure 9; Table A2).

Taking the karst area as an example, since the implementation of ecological projects, soil accumulation quickly recovered after abandoned farmland evolved into grassland and shrubland (Liu et al. 2020). Therefore, scholars believed that increasing vegetation coverage could play a key role in reducing nitrogen deposition in local ecosystems (Han et al. 2015). The research results were consistent with them. Improved the quality of cultivated field and grassland may greatly improve the synergy relationship of ES and promote the well development of the ecological environment.

4.2. Comparisons of the results with that in previous studies

We compared our results with previous researches. In terms of ecosystem service, The Ordos City had a total area of $8.68 \times 10^4 \text{ km}^2$, the average value of SC was 47.79

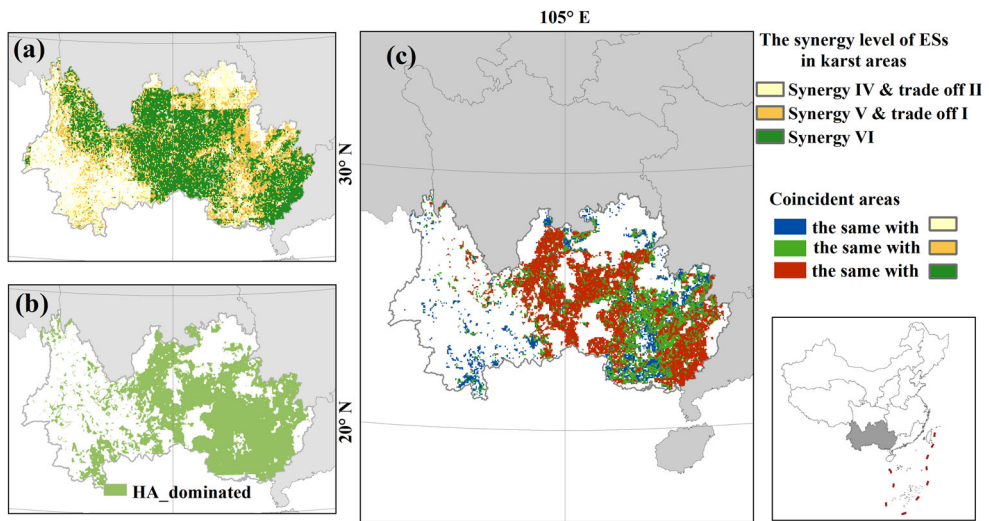


Figure 7. The synergy level of ESs in karst areas. (a) The synergy level of ESs diagram in karst areas; (b) vegetation restoration contributed by human activities; (c) the overlapping space between the human activities control areas and the multi-ESs synergy area.

Table 3. Changes in areas of land use types from 1992 to 2015 (10^4 km^2).

Land use type	Area						Before returning farmland to forests	After returning farmland to forests	Total area transformation	Total rate of change
	1992	1995	2000	2005	2010	2015	1992–2000	2000–2015		
Cultivated field	270.58	271.73	275.82	274.63	274.48	272.86	5.24	-2.96	2.28	0.8%
Woodland	183.55	182.79	181.68	182.75	182.33	182.27	-1.87	0.59	-1.28	-0.7%
Grassland	299.43	298.52	296.86	296.34	296.22	296.61	-2.56	-0.26	-2.82	-0.9%
Wetlands	3.44	3.44	3.49	3.59	3.66	3.68	0.05	0.19	0.24	6.9%
Urban land	3.49	3.81	4.37	7.01	9.62	12.31	0.88	7.94	8.83	253%
Unutilized land	190.32	190.53	188.53	186.41	184.39	182.87	-1.80	-5.66	-7.45	-3.9%
Waters	12.64	12.61	12.68	12.70	12.74	12.85	0.04	0.17	0.21	1.7%

$\text{t}\cdot\text{hm}^{-2}\text{yr}^{-1}$ and $59.04 \text{ t}\cdot\text{hm}^{-2}\text{yr}^{-1}$ in 2000 and 2010, respectively (Wu et al. 2017). The Jiayu city of Gansu Province had a total area of $1.94 \times 10^5 \text{ km}^2$. The average value of SC increased from $24.14 \text{ t}\cdot\text{hm}^{-2}\text{yr}^{-1}$ in 2000 to $44.42 \text{ t}\cdot\text{hm}^{-2}\text{yr}^{-1}$ in 2010, and the total amount had increased from 6524.59 tons to 11,988.57 tons (Pan and Li 2017). Taihu Lake Basin covers an area over $3.69 \times 10^4 \text{ km}^2$, the SC was $3.38 \times 10^3 \text{ t}\cdot\text{km}^{-2}\text{yr}^{-1}$ in 2000 (Qiao et al. 2019). Relevant scholars had conducted geographic statistical analysis on a large number of field sample data and found that the soil and water conservation and water transfer capabilities had gradually increased in karst areas (Nie et al. 2012). Our research results were consistent with it. However, some researchers had reached different conclusions, for example, the areas of the trade-offs between SC and NPP was larger than synergies in the Han River Basin of China (Wang et al. 2017). In this research, the overall SC and NPP showed synergies in the Loess Plateau (Figure 5), but there were still trade-offs in some areas from the spatial map (Figure 4). Previous scholars had found that 84.4% of the SC occurred on the slopes between 8° and 35° after the restoration of vegetation on the Loess Plateau (Lü et al. 2012). the average erosion rate in areas with slopes

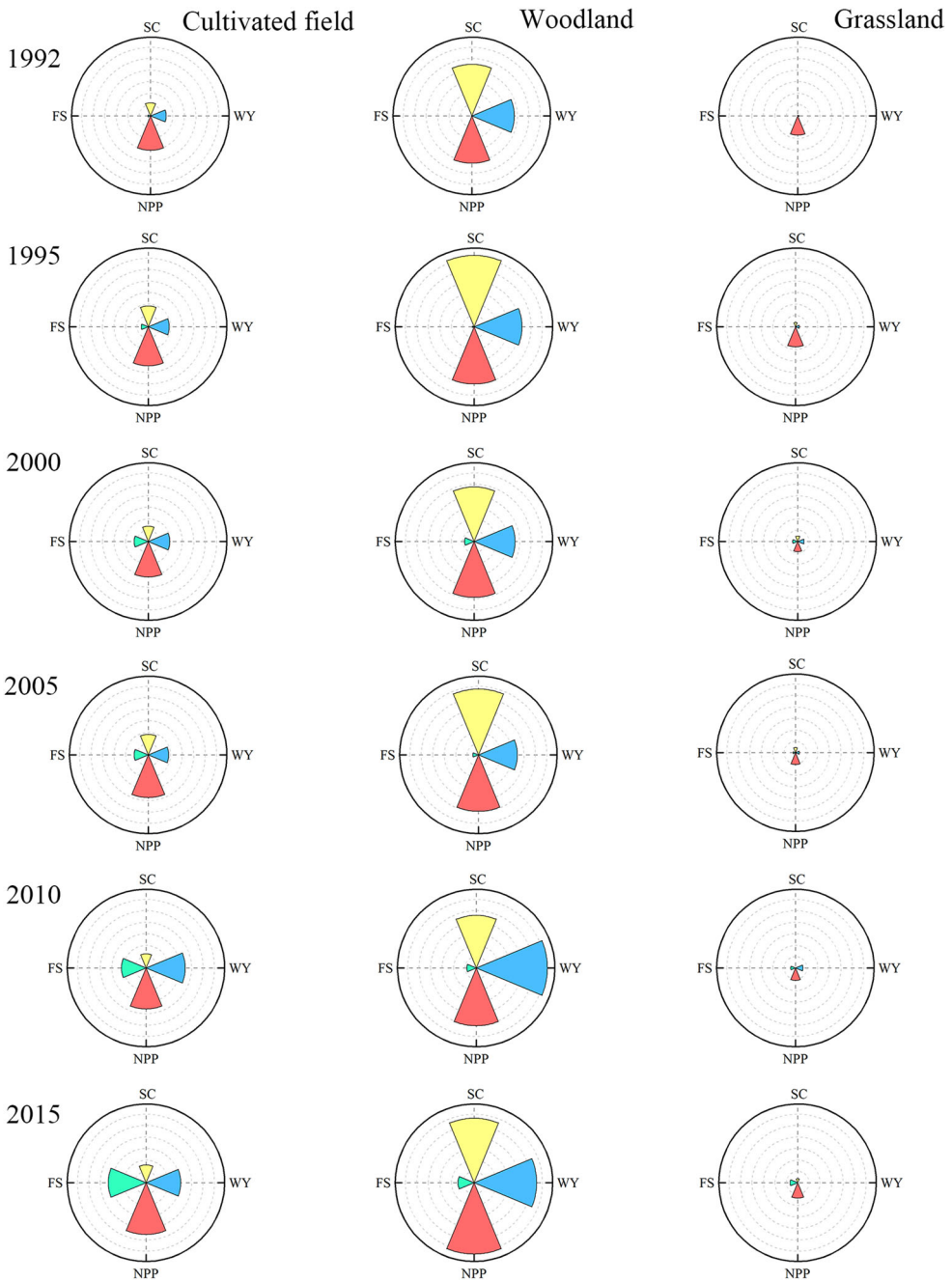


Figure 8. Rose chart of the dynamic change of ES mean in different land types from 1992 to 2015.

exceeding 8° was far exceeded the allowable erosion rate (Cai 2001). Our results were consistent with it. These require us to clarify specific spatial scales when studying the relationship of ESs in order to make scientific and reasonable ecological management decisions.

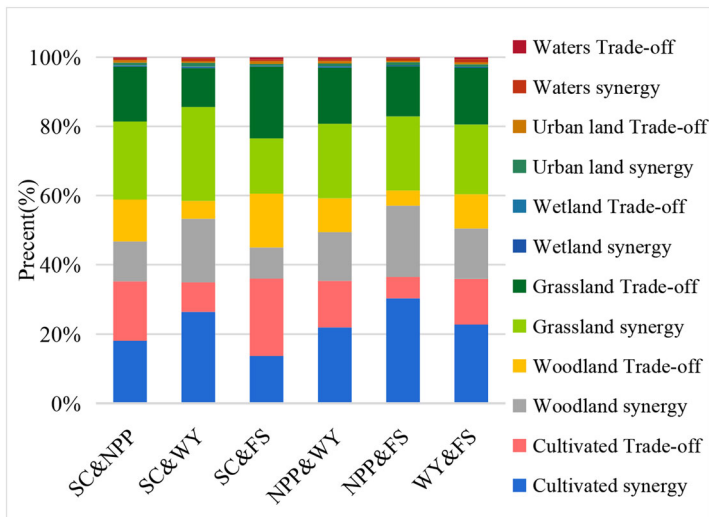


Figure 9. Histogram of the proportion of trade-offs and synergies of ESs in different land types.

4.3. Ecological engineering promotes multi-ESs synergy in SW karst areas

The ecological environment in Karst areas is fragile, with serious land degradation (Yuan 1993), the impact on NPP is mainly reflected in the lack of soil, insufficient soil nutrients, and low soil surface water, which is not conducive to vegetation growth. In terms of climate, the SW karst region is affected by the confluence of the southeast monsoon and northwest cold wind, with large cloud cover and insufficient solar radiation, which is also unfavorable to local vegetation growth. In recent years, the growth of NPP has mainly relied on the positive impact of human activities (mainly ecological engineering) on it. The implementation of the ‘Return farmland to forest’ project and the comprehensive control of rocky desertification in Southwest China have caused tremendous changes in land types (Geng et al. 2006; Liu et al. 2018). The vegetation cover rapidly increased 7% over the karst areas from 1999 to 2012 (Brandt et al. 2018a). By the end of 2016, the area of rocky desertification land will be reduced by an average of 3864 km² per year compared with 2011. These results clearly indicated that the ecological environment had improved in SW karst areas (Mu 2019).

In this article, we through trend analysis and abrupt year test (Figure 6(e)) to confirmed that NDVI (Normalized Vegetation Index) showed an upward trend in SW karst areas (Figure 6(a)). Second, we further determined the main influencing factors affecting vegetation restoration in the Southwest Karst region, calculated according to the four designed scenarios in Table 2, which confirms that the vegetation restoration in southwest karst area was mainly contributed by HA. Third, we proved that the vegetation restoration by HA (mainly ecological engineering) plays a key role for synergies among multi-ESs synergy in SW karst areas. The above is the main impact of HA on the growth of NPP. In terms of climate factors, precipitation showed a positive contribution in NDVI coverage in the karst region of China (Wu et al. 2020). Temperature variation is positively correlated with NPP (Ran et al. 2020), the raised temperature increases NPP by enhancing photosynthesis. In this study, precipitation and temperature were in increased trend before and after the mutation year, but the growth rate of precipitation was faster than the temperature (Figure 6(f,g)), and these promoted the rise of WY and NPP.

In terms of SC, the increase in rainfall in the SW will lead to an increase in rainfall erosivity, which will have a negative impact on the soil conservation. However, the vegetation coverage maintains the local soil conservation to a certain extent due to the role of ecological protection projects. WY is mainly related to rainfall and evapotranspiration. Studies have confirmed that the varied precipitation and temperature play an important role during the process of soil conservation, water yield, and NPP changes (Ran et al. 2020). Temperature will affect the rate of vegetation transpiration and water evaporation to a certain extent, the growth rate of precipitation faster than the temperature in SW karst areas (Figure 6(f,g)), so the WY was also an upward trend. For FS, economic backwardness directly or indirectly causes farmers to reclaim slopes to grow crops in Karst mountain areas and destroy considerable forest resources, An increase in grain yield is often at the cost of soil erosion intensification and runoff increase (Tian et al. 2016). The output of agricultural products and forest products has continued to rise. With the control of rocky desertification of cultivated land, regional vegetation coverage has increased in the SW karst areas in recent years. According to the data obtained in the China Statistical Yearbook, the food production and food value of the SW Karst region (Guizhou, Yunnan and Guangxi provinces) were obtained, as shown in Table A3. That is, all ESs showed a synergy upward trend.

Previous scholars had confirmed that the increase of NDVI could promote the SC and NPP (Peng et al. 2011; Cai et al. 2014; Xiao 2014; Zhang et al. 2016; Li et al. 2016). HA plays an important role in vegetation restoration by changing land use structure (Piao et al. 2009). Chang et al. (2012) speculated that a high SC amount indicates minimal free water flow, good water conservation, and high vegetation carbon fixation. In this study, SC and NPP showed a synergistic relationship, which was inseparable from the growth of vegetation coverage. The increase in WY was due to the combined effect of vegetation coverage and rainfall conditions. The increase of FS was mainly related to the management of environmental problems and the increase in vegetation coverage. All in all, the four ESs all present a synergistic relationship of the SW karst area, which was directly related to the driving factor of vegetation coverage. Finally, we also corroborated our research results through the research and reports of other scholars, ecological restoration measures implemented were the main influencing factors for synergies of ESs in SW karst areas. Our results were consistent with the findings of related studies (Hou et al. 2015; Zhang et al. 2018). Therefore, the areas of synergies among multi-ESs should become the key areas for ecological restoration, so as to promote the synergy of ESs.

4.4. Limitations and future study directions

This article separately discusses the correlation of ES in the nine agricultural areas taking into the heterogeneity of geographic space. In addition, it must be noted that in order to unify the resolution of the four ESs after analyzing the spatial distribution, 0.05° raster data was used for evaluation, which leads to the study of FS was 30.25 times larger compared to other $1\text{ km} \times 1\text{ km}$ resolution studies, due to the difference in cultivated field, woodland, grassland and water, it will also cause a large difference in the amount of FS per unit area of water and cultivated field in China's provinces and cities. If we want to provide better ecological guidance for the future, this article should make progress in the following aspects: collect data sources with finer resolution; explore the dynamic changes and influencing factors of ESs trade-offs and synergies based on different scales, and

provide scientific decision-making references based on ESs interrelationships in different regions; Consider the multiple interactions between human society and ecosystems (Ellis and Ramankutty 2008), such as accumulation of organic pollutants (Renard et al. 2015). These studies will improve human well-being and our ability to adapt to changes in the ecological environment in a more comprehensive and credible way. In the future, we will further consider what is the most effective way to weaken or reverse trade-offs and enhance synergy of ESs, and whether the correlation between ESs is strong, and how the strength of this relationship changes over time, management and scale, and the flow of ecosystem services and the relationship between supply and demand.

5 Conclusion

The study evaluated ES trade-offs and synergies in China, revealed its spatiotemporal evolution as well as spatial heterogeneity, and identified the synergies among multi-ESs areas. Besides, We explored the impact of human activities on vegetation restoration and ecological engineering on trade-offs and synergies, the following conclusions were got after studying: (1) All ESs had increased in China, the SW karst areas contributed 23.7% of SC, 14.56% of NPP and 14% of WY with only 8.4% of China's continent; (2) SC and WY showed a synergy in 73.21% of China's areas, the SW karst areas, Sichuan Basin, and southern China showed synergistic of all ESs, but the synergy of ESs was the strongest in SW karst areas; (3) 49.28% of China's continent was synergy control areas of multi-ESs, while accounted for 82.23% in SW karst areas, the synergy control areas were regarded as areas where ecological restoration projects could achieve significant benefits; (4) The synergy among multi-ESs in SW karst areas was the result of joint efforts of precipitation, temperature, and ecological restoration projects, but the ecological restoration project was the main reason. The coverage of NDVI was obviously increased after the mutation year, and it was mainly due to human activities (HA). Most importantly, the coincidence rate between the HA dominated areas and the synergies among multi-ESs areas was as high as 90.7%, these proved that ecological engineering had played a key role for synergies among multi-ESs in SW karst areas; (5) The synergy of ESs areas was concentrated in cultivated field and grassland, all ESs have increased in cultivated field and woodland. Woodland was the main provider of ES, and its contribution to SC, NPP, and WY reached 54%, 40%, and 37%, respectively. It was crucial to identify the priority areas that lead to synergies among multiple ESs, to promote the healthy development of the ecological environment.

Author contributions

Conceptualization, Xiaoyong Bai; Data curation, Min Liu and Luhua Wu; Formal analysis, Min Liu and Cuiwei Zhao; Investigation, Min Liu; Methodology, Min Liu and Qiu Tan; Validation, Min Liu, Guangjie Luo and Chen Ran; Visualization, Min Liu and Yuanhong Deng; Writing—original draft, Min Liu; Writing—review & editing, Min Liu, Luhua Wu, Zeyin Hu and Chen Ran. All authors have read and agreed to the published version of the manuscript.

Disclosure statement

The authors declare that they have no known competing financial interests or personal relationships that could have appeared to influence the work reported in this article.

Funding

This research work was supported jointly by the Strategic Priority Research Program of the Chinese Academy of Sciences (No. XDB40000000 and No. XDA23060100), National Natural Science Foundation of China (No. 42077455), Western Light Talent Program (Category A) (No. 2018-99), United fund of karst science research center (No. U1612441).

ORCID

Xiaoyong Bai  <http://orcid.org/0000-0001-9705-5574>

References

- Bai Y, Ouyang Z, Zheng H, Li X, Zhuang C, Jiang B. 2012. Modeling soil conservation, water conservation and their tradeoffs: a case study in Beijing. *J Environ Sci.* 24(3):419–426.
- Bai Y, Wong CP, Jiang B, Hughes AC, Wang M, Wang Q. 2018. Developing China's Ecological Redline Policy using ecosystem services assessments for land use planning. *Nat. Commun.* 9:3034.
- Brandt M, Yue Y, Wigneron JP, Tong X, Tian F, Jepsen MR, Xiao X, Verger A, Mialon A, Al-Yaari A, et al. 2018. Satellite-observed major greening and biomass increase in South China Karst during recent decade. *Earth Future* 6(7):1017–1028.
- Barbier EB, Koch EW, Silliman BR, Hacker SD, Wolanski E, Primavera J, Granek EF, Polasky S, Aswani S, Cramer LA, et al. 2008. Coastal ecosystem-based management with nonlinear ecological functions and values. *Science* 319(5861):321–323.
- Bennett EM, Peterson GD, Gordon LJ. 2009. Understanding relationships among multiple ecosystem services. *Ecol Lett.* 12(12):1394–1404.
- Cai H, Yang X, Wang K, Xiao L. 2014. Is forest restoration in the Southwest China Karst promoted mainly by climate change or human-induced factors? *Remote Sens.* 6(10):9895–9910.
- Cai QG. 2001. Soil erosion and management on the Loess Plateau. *J Geog Sci.* 11(1):53–70.
- Cai C, Ding S, Shi Z, Huang L, Zhang G. 2000. Study of applying USLE and geographical information system IDRISI to predict soil erosion in small watershed. *Soil Water Conserv.* 14:19–24. (in Chinese).
- Chang R, Fu B, Liu G, Wang S, Yao X. 2012. The effects of afforestation on soil organic and inorganic carbon: a case study of the Loess Plateau of China. *Catena* 95:145–152.
- Chen C, Park T, Wang X,H, Piao SL, Xu B,D, Chaturv RK, Richard F, Victor B, Ciais P, Rasmus F, et al. 2019. China and India lead in greening of the world through land-use management. *Nat Sustain.* 2(2): 122–129.
- Chen P. 2019. Monthly net primary productivity of China's terrestrial ecosystem 1 km grid dataset (18–2015) north of North Latitude (1985–2015) [DB/OL]. Global Change Science Research Data Publishing System. <http://doi.org/10.3974/geodb.2019.03.02.V1>.
- Costanza R, d'Arge R, de Groot R, Farber S, Grasso M, Hannon B, Limburg K, Naeem S, O'Neill RV, Paruelo J, et al. 1997. The value of the worlds ecosystem services and natural capital. *Nature* 387(6630):253–260.
- Diaz RJ, Rosenberg R. 2008. Spreading dead zones and consequences for marine ecosystems. *Science.* 321(5891):926–929.
- Ellis EC, Ramankutty N. 2008. Putting people in the map: anthropogenic biomes of the world. *Front Ecol Environ.* 6(8):439–447.
- Forzieri G, Miralles DG, Ciais P, Alkama R, Ryu Y, Duveiller G, Zhang K, Robertson E, Kautz M, Martens B, et al. 2020. Increased control of vegetation on global terrestrial energy fluxes. *Nat Clim Chang.* 10(4):356–362.
- Geng XQ, Zhu MQ, Jiang ZC. 2006. Research progress of karst rocky desertification in Southwest China in recent years. *Carsol Sin.* 3:234.
- Goldstein JH, Caldarone G, Duarte TK, Ennaanay D, Hannahs N, Mendoza G, Polasky S, Wolny S, Daily GC. 2012. Integrating ecosystem-service tradeoffs into land-use decisions. *Proc Natl Acad Sci USA* 109(19):7565–7570.
- Gong S, Xiao Y, Zheng H, Xiao Y, Ouyang Z. 2017. Spatial characteristics of water conservation in Chinese ecosystems and their influencing factors. *Acta Ecol Sin.* 37 (07):2455–2462.

- Guerry AD, Polasky S, Lubchenco J, Chaplin-Kramer R, Daily GC, Griffin R, Ruckelshaus M, Bateman JJ, Duraipapp A, Elmqvist T, et al. **2015**. Natural capital and ecosystem services informing decisions: from promise to practice. *Proc Natl Acad Sci USA* 112(24):7348–7355.
- Hou WJ, Gao JB, Wu SH, Dai E. **2015**. Interannual variations in growing-season NDVI and its correlation with climate variables in the southwestern karst region of China. *Remote Sens.* 7 (9):11105–11124.
- Howe C, Suich H, Vira B, Mace GM. **2014**. Creating win-wins from trade-offs? Ecosystem services for human well-being: A meta-analysis of ecosystem service trade-offs and synergies in the real world. *Global Environ Change* 28:263–275.
- Hu Z, Wang S, Bai X, Luo G, Li Q, Wu L, Yang Y, Tian S, Li C, Deng Y. **2020**. Changes in ecosystem service values in karst areas of china. *Agricult Ecosyst Environ.* 301:107026.
- Jain HK. **2010**. Green revolution: history impact and future. *Indian J Genet Plant Breed* (4).
- Jiang C, Li DQ, Wang DW, Zhang LB. **2016**. Quantification and assessment of changes in ecosystem service in the Three-River Headwaters Region, China as a result of climate variability and land cover change. *Ecol Indic.* 66:199–211.
- Joppa LN, Boyd JW, Duke CS, Hampton S, Jackson ST, Jacobs KL, Kassam KS, Mooney HA, Ogden LA, Ruckelshaus M, et al. **2016**. Government: plan for ecosystem services. *Science* 351(6277):1037–1037.
- Lai L, Huang X, Yang H, Chuai X, Zhang M, Zhong T, Chen Z, Chen Y, Wang X, Thompson JR. **2016**. Carbon emissions from land-use change and management in China between 1990 and 2010 *Sci Adv.* 2(11):e1601063.
- Lele S, Springate-Baginski O, Lakerveld R, Deb D, Dash P. **2013**. Ecosystem services: origins, contributions, pitfalls, and alternatives. *Conservat Soc.* 11(4):343–358. www.jstor.org/stable/26393131.
- Li S, Liang W, Fu BJ, Lü YH, Fu SY, Wang S, Su HM. **2016**. Vegetation changes in recent large-scale ecological restoration projects and subsequent impact on water resources in China's Loess Plateau. *Sci Total Environ.* 569–570:1032–1039.
- Li SC, Zhang CY, Liu JL, Zhu WB, Ma C, Wang J. **2013**. The tradeoffs and synergies of ecosystem services: research progress, development trend, and themes of geography. *Geogr Res.* 32 (2013) :1379–1390.
- Liu J, Han G. **2020**. Major ions and $\delta^{34}\text{S}\text{SO}_4$ in Jiulongjiang River water: investigating the relationships between natural chemical weathering and human perturbations. *Sci Total Environ.* 724:138208
- Liu BY, Nearing MA, Shi PJ, Jia ZW. **2000**. Slope gradient effects on soil loss for steep slopes. *Soil Sci Soc Am J.* 64(5):1759–1763.
- Liu M, Han G, Zhang Q. **2020**. Effects of agricultural abandonment on soil aggregation, soil organic carbon storage and stabilization: Results from observation in a small karst catchment, Southwest China. *Agricult Ecosyst Environ.* 288:106719.
- Liu YX, Lü YH, Fu B, Harris P, Wu L. **2018**. Quantifying the spatio-temporal drivers of planned vegetation restoration on ecosystem services at a regional scale. *Sci Tot Environ.* 650:102.
- Lü YJ, Fu BJ, Feng XM, Zeng Y, Liu Y, Chang RY, Sun G, Wu BF. **2012**. A policy-driven large scale ecological restoration: quantifying ecosystem services changes in the Loess Plateau of China. *PLoS One* 7(2):e31782.
- MA (Millennium Ecosystem Assessment). **2005**. *Ecosystems and Human Well-Being: current state and trends: Synthesis*. Washington, DC: Island Press; p. 829–838.
- McCool DK, Foster GR, Mutchler CK, Meyer LD. **1989**. Revised slope length factor for the universal soil loss equation. *Trans ASAE.* 32:1571–1576.
- Mouchet MA, Lamarque P, Martín-López B, Crouzat E, Gos P, Byczek C, Lavorel S. **2014**. An interdisciplinary methodological guide for quantifying associations between ecosystem services. *Global Environ Change* 28:298–308.
- Mu HX. **2019**. Benefits evaluation of integrated control of the rocky desertification in southwest karst area [dissertation]. Beijing Forestry University.
- Nie YP, Chen HS, Wang KL, Yang J. **2012**. Water source utilization by woody plants growing on dolomite outcrops and nearby soils during dry seasons in karst region of southwest china. *J Hydrol.* 420-421(4):264–274.
- Ouyang Z, Wang X, Miao H. **1999**. A preliminary study on the service functions of terrestrial ecosystems in China and their eco-economic value. *Acta Ecol Sin.* (05):19–25.
- Ouyang Z, Zheng H, Xiao Y, Polasky S, Liu JG, Xu WH, Wang Q, Zhang L, Xiao Y, Rao E, et al. **2016**. Improvements in ecosystem services from investments in natural capital. *Science* 352(6292):1455–1459.,

- Palm CA, Smukler SM, Sullivan CC, Mutuo PK, Nyadzi GI, Walsh MG. 2010. Identifying potential synergies and trade-offs for meeting food security and climate change objectives in sub-Saharan Africa. *Proc Natl Acad Sci USA* 107(46):19661–19666.
- Pan JH, Li Z. 2017. Analysis on trade-offs and synergies of ecosystem services in arid inland river basin. *Trans Chin Soc Agric Eng.* 33(17):280–289.
- Pan MH, Wu YQ, Ren PP. 2010. Estimation of soil erosion in Dongjiang river basin based on USLE. *J Nat Resour.* 5(12):2154–2164.
- Pan Y, Xu ZR, Wu JX. 2013. Spatial differences of the supply of multiple ecosystem services and the environmental and land use factors affecting them. *Ecosyst Serv.* 5:4–10.
- Peng J, Hu XX, Wang X, Meersmans J, Liu YX, Qiu SJ. 2019. Simulating the impact of Grain-for-Green Programmed on ecosystem services trade-offs in Northwestern Yunnan, China. *Ecosyst Serv.* 39: 100998.
- Peng SS, Chen AP, Xu L, Cao CX, Fang JY, Myneni RB, Pinzon JE, Tucker CJ, Piao SL. 2011. Recent change of vegetation growth trend in China. *Environ Res Lett.* 6(4):044027.
- Piao S, Fang J, Ciais P, Peylin P, Huang Y, Sitch S. 2009. The carbon balance of terrestrial ecosystems in china. *China Basic Ence.* 458(7241):1009–1013.
- Potter CS, Randerson JT, Field CB, Matson PA, Vitousek PM, Mooney HA, Klooster SA. 1993. Terrestrial ecosystem production: A process model based on global satellite and surface data. *Global Biogeochem Cycles* 7(4):811–841.
- Qiao X, Gu Y, Zou C, Xu D, Wang L, Ye X, Yang Y, Huang XF. 2019. Temporal variation and spatial scale dependency of the trade-offs and synergies among multiple ecosystem services in the Taihu lake basin of China. *Sci Total Environ.* 651(Pt 1):218–229.
- Qin KY, Li J, Yang XN. 2015. Trade-off and synergy among ecosystem services in the Guanzhong-Tianshui economic region of China. *Int J Environ Res Public Health* 12(11):14094–14113.
- Ran C, Wang S, Bai X, Luo G, Zhao C, Tan Q, Luo X, Chen H, Xi H. 2020. Trade-offs and synergies of ecosystem services in Southwestern China. *Environ Eng Sci.* 37(10):669–678.
- Ran F, Luo Z, Wu J, Qi S, Cao L, Cai Z, Chen Y. 2019. Spatiotemporal pattern of trade-offs and synergies of ecosystem services in Poyang Lake area. *Chin J Appl Ecol.* 30 (03):995–1004.
- Renard D, Rhemtulla JM, Bennett EM. 2015. Historical dynamics in ecosystem service bundles. *Proc Natl Acad Sci USA* 2015:02565.
- Renard KG, Foster GR, Weesies GA, McCool DK, Yoder DC. 1997. Predicting soil erosion by water: A guide to conservation planning with the revised universal soil loss equation (RUSLE). USDA, Agricultural Handbook Number 703. Washington, D.C.: U.S. Government Printing Office.
- Santiago MM, José Luis MG. 2019. Land-change dynamics and ecosystem service trends across the central high-Andean Puna. *Sci Rep.* 9(1).
- Simonit S, Perrings C. 2013. Bundling ecosystem services in the Panama Canal watershed. *Proc Natl Acad Sci USA.* 110(23):9326–9331.
- Slayback DA, Pinzon JE, Los SO, Tucker CJ. 2003. Northern hemisphere photosynthetic trends 1982–99. *Global Change Biology.* 9(1):1–15.
- Han G, Tang Y, Liu M, Van Zwieten L, Yang X, Yu C, Wang H, Song Z. 2020. Carbon-nitrogen isotope coupling of soil organic matter in a karst region under land use change, Southwest China. *Agric Ecosyst Environ.* 301:107027.
- Sun Y, Li J, Liu X, Ren Z, Zhou Z, Duan Y. 2020. Spatially explicit analysis of trade-offs and synergies among multiple ecosystem services in Shaanxi Valley Basins. *Forests* 11(2):209.
- Sun W, Shao Q, Liu J, Zhai J. 2014. Assessing the effects of land use and topography on soil erosion on the Loess Plateau in China. *Catena* 121:151–163.
- Sun Y, Ren Z, Hao M. 2019. Spatiotemporal changes and influencing factors of trade-offs and synergies in ecosystem services on the Loess Plateau: A case study of Yanan City. *Chin J Ecol.* (10):3443–3454.
- Tian Y, Wang S, Bai X, Luo G, Xu Y. 2016. Trade-offs among ecosystem services in a typical Karst watershed, SW China. *Sci Total Environ.* 566:1297–1308.
- Tifafi M, Guenet B, Christine H. 2017. Large differences in global and regional total soil carbon stock estimate based on Soil Grids, HWSD and NCSCD: Inter comparison and evaluate based on field data from USA, England, Wales and France. *Global Biogeochem Cycles.* (15):42–56. <https://doi.org/10.1002/2017GB005678>.
- Tong X, Wang K, Yue Y, Brandt M, Liu B, Zhang C, Liao C, Fensholt R. 2017. Quantifying the effectiveness of ecological restoration projects on long-term vegetation dynamics in the karst regions of southwest China. *Int J Appl Earth Obser Geoinformation.* 54:105–113.

- Tong XW, Brandt M, Yue YM, Horion S, Wang KL, Keersmaecker WD, Tian F, Schurgers G, Xiao XM, Luo YQ, et al. 2018. Increased vegetation growth and carbon stock in China karst via ecological engineering. *Nat Sustain.* 1(1):44–50.
- Turner KG, Odgaard MV, Bøcher PK, Dalgaard T, Svenning JC. 2014. Bundling ecosystem services in Denmark: Trade-offs and synergies in a cultural landscape. *Landscape Urban Plann.* 125:89–104.
- Wang B, Zhao J, Hu XF. 2016. Spatial pattern analysis of ecosystem services in Heihe River basin based on InVEST model. *Chin J Ecol.* 35 (10):2783–2792.
- Wang P, Zhang L, Li Y, Jiao L, Fu BJ. 2017. Spatio-temporal characteristics of the trade-off and synergy relationships among multiple ecosystem services in the upper reaches of Hanjiang river basin. *J Geograph Ences.* 72(11):2064–2078.
- Wu JX, Zhao Y, Yu CQ, Luo LM, Pan Y. 2017. Land management influences trade-offs and the total supply of ecosystem services in alpine grassland in Tibet, China. *J Environ Manage.* 193:70–78.
- Wu L, Wang S, Bai X, Luo W, Tian Y, Zeng C, Luo G, He S. 2017. Quantitative assessment of the impacts of climate change and human activities on runoff change in a typical karst watershed, SW China. *Sci Total Environ.* 601-602:1449–1465.
- Wu L, Wang S, Bai X, Luo W, Tian Y, Zeng C, Luo G, Wang J, Li Q, Chen F, et al. 2020. Climate change weakens the positive effect of human activities on karst vegetation productivity restoration in southern China. *Ecol Indic.* 115:106392.
- Wu WH, Peng J, Liu YX, Hu YN. 2017. Tradeoffs and synergies between ecosystem services in Ordos City. *Prog Geogr.* 36(12):1571–1581.
- Wischmeier WH. 1971. A soil erodibility nomograph for farmland construction sites. *J Soil Water Conserv.* 26:189–193.
- Williams JR, Arnold JG. 1997. A system of erosion: Sediment yield models. *Soil Technol.* 11(1):43–55.
- Xiao JF. 2014. Satellite evidence for significant biophysical consequences of the ‘Grain for Green’ Program on the Loess Plateau in China. *J Geophys Res Biogeosci.* 119(12):2261–2275.
- Xu X, Yang G, Tan Y, Liu J, Hu H. 2018. Ecosystem services trade-offs and determinants in China’s Yangtze River Economic Belt from 2000 to 2015. *Sci Tot Environ.* 634:1601–1614.
- Yang S, Zhao W, Liu Y, Wang S, Wang J, Zhai R. 2018. Influence of land use change on the ecosystem service trade-offs in the ecological restoration area: Dynamics and scenarios in the Yanhe watershed, China. *Sci Total Environ.* 644:556–566
- Yang Y, Wang S, Bai X, Tan Q, Li Q, Wu LH, Tian SQ, Hu ZY, Li CJ, Deng YH. 2019. Affecting long-term trends in global NDVI. *Factors* 10(5):372.
- Yuan DX. 1993. *China karstology.* Beijing: Geological Publishing House. p. 1–3.
- Zeng C, Wang S, Bai X, Li Y, Tian Y, Li Y, Wu LH, Luo GJ. 2017. Soil erosion evolution and spatial correlation analysis in a typical karst geomorphology using RUSLE with GIS. *Solid Earth* 8(4):721–736.
- Zhang M, Wang K, Liu H, Zhang C, Yue Y, Qi X. 2018. Effect of ecological engineering projects on ecosystem services in a karst region: a case study of northwest Guangxi, China. *J Clean Prod.* 183: 831–842.
- Zhang Y, Peng C, Li W, Tian L, Zhu Q, Chen H, Fang X, Zhang G, Liu G, Mu X, et al. 2016. Multiple afforestation programs accelerate the greenness in the ‘Three North’ region of China from 1982 to 2013. *Ecol Indic.* 61:404–412.
- Zhang L, Hickel K, Dawes WR, Chiew FHS, Western AW, Briggs PR. 2004. A rational function approach for estimating mean annual evapotranspiration. *Water Resour Res.* 40(2):W02502.
- Zheng H, Wang L, Peng W, Zhang C, Li C, Robinson BE, Wu X, Kong L, Li R, Xiao Y, et al. 2019. Realizing the values of natural capital for inclusive, sustainable development: Informing China’s new ecological development strategy. *Proc Natl Acad Sci USA.* 116(17):8623–8628.
- Zhou L, Tucker CJ, Kaufmann RK, Slayback D, Shabanov NV, Myneni RB. 2001. Variations in northern vegetation activity inferred from satellite data of vegetation index during 1981 to 1999. *J Geophys Res.* 106(D17). <https://doi.org/10.1029/2000JD000115>.

Appendix A

Table A1. The average of ES in nine agricultural divisions from 1992 to 2015.

	SC ($\text{t}\cdot\text{hm}^{-2}\cdot\text{yr}^{-1}$)			NPP ($\text{g}\cdot\text{C}\cdot\text{m}^{-2}\cdot\text{yr}^{-1}$)			WY (10^6m^3)			FS ($10^7\text{t}\cdot\text{ha}^{-1}$)		
	1992	2015	Changed	1992	2015	Changed	1992	2015	Changed	1992	2015	Changed
Northeast China Plain	63.38	62.61	-0.77	245.41	307.11	61.7	1.89	1.67	-0.23	0.56	0.59	0.032
Northern arid and semiarid region	14.53	15.45	0.92	131.89	111.25	-20.64	1.02	0.89	-0.12	0.012	0.02	0.007
Huang-Huai-Hai Plain	60.62	61.23	0.61	201.1	288.38	87.28	2.06	2.48	0.43	704.51	796.43	91.91
Loess Plateau	117.16	76.72	-40.44	241.65	289.71	48.06	2.78	1.29	-1.49	0.016	0.043	0.026
Qinghai Tibet Plateau	89.71	131.05	41.34	127.93	126.08	-1.85	3.31	3.52	0.21	0.0004	0.0009	0.0005
Middle-lower Yangtze Plain	245.07	271.48	26.41	267.41	360.23	92.82	11.16	19	7.84	3368	3420	51.48
Sichuan Basin and surrounding regions	309.12	442.09	132.97	277.22	341.99	64.77	4.90	5.88	0.98	7.29	7.33	0.036
Karst areas in southwest China	387.24	457.06	69.82	294.76	449.55	154.79	4.53	13.31	8.78	0.36	0.37	0.01
Southern China	521.79	741.69	219.9	339.64	481.25	141.61	27.07	26.61	-0.46	116.87	108.07	-8.80

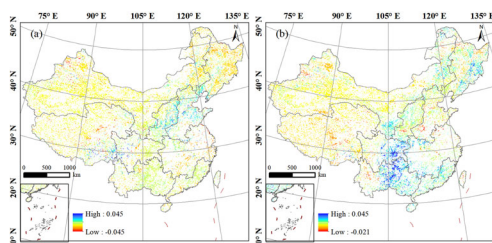


Figure A1. The spatial distribution of NDVI in first stage trend (a) and second stage trend (b). Division of the counties into four groups according to their total area of conservation projects.

Table A2. The proportion of ES synergy in various categories from 1992 to 2015.

Land use type, ES	SC & NPP	SC & WY	SC & FS	NPP & WY	NPP & FS	WY & FS
Cultivated field	18.08%	26.44%	13.69%	21.94%	30.37%	22.77%
Woodland	11.46%	18.30%	8.88%	13.99%	20.51%	14.49%
Grassland	22.58%	27.16%	15.97%	21.52%	21.44%	20.18%
Wetlands	0.21%	0.29%	0.14%	0.24%	0.20%	0.15%
Urban land	0.75%	1.07%	0.47%	0.80%	0.93%	0.74%
Waters	0.47%	0.81%	0.48%	0.59%	0.71%	0.89%

TABLE A3. The food production and food value of the SW Karst region in 1992 and 2015.

Year	1992				1992 (100 million yuan)			
	Agricultural output (10,000 tons)	Forestry output (10,000 m ³)	Animal husbandry output (10,000 tons)	Fishery (10,000 tons)	Agricultural output value	Forestry output value	Animal husbandry output value	Fishery output value
Guizhou	788.9	136	85.5	2.36	116.03	12.22	47.18	1.3
Yunnan	1070.4	745	92.2	5.37	163.93	22.84	61.56	2.02
Guangxi	1418.9	328	136.2	44.57	188.65	26.77	100.72	16.99
Total	3278.2	1209	313.9	52.3	468.61	61.83	209.46	20.31
Year	2015 (100 million yuan)							
Areas	Agricultural output (10,000 tons)	Forestry output (10,000 m ³)	Animal husbandry output (10,000 tons)	Fishery (10,000 tons)	Agricultural output value	Forestry output value	Animal husbandry output value	Fishery output value
Guizhou	1210.57	175	201.94	24.98	1773.72	137.7	667.14	55.06
Yunnan	1791.27	348	378.31	69.71	1794.65	317.12	1147.53	67.62
Guangxi	1433.15	2106	417.27	345.92	2146.37	313.9	1140.3	429.82
Total	4434.99	2629	997.52	440.61	5714.74	768.72	2954.97	552.5